Journal of Electronic Imaging 17(4), 043025 (Oct–Dec 2008)

Image-based evaluation of seam puckering appearance

Binjie Xin
Hong Kong Polytechnic University
Institute of Textiles and Clothing
Hung Hom, ST611
Hong Kong, 852

George Baciu
Hong Kong Polytechnic University
Department of Computing
Hong Kong, 852

Jinlian Hu
Hong Kong Polytechnic University
Institute of Textiles and Clothing
Hung Hom, ST611
Hong Kong, 852
E-mail: tchujl@inet.polyu.edu.hk

Abstract. *We present the development of an objective evaluation method based on the integration of X-illumination, morphological fractal analysis and Bayes classifier that aims at characterizing the seam-puckering appearance. The experimental results in our research demonstrate that a highly significant correlation coefficient can be achieved between the estimated grades and the technician-generated grades; the presented method is insensitive to the color/texture of fabrics, thus showing the potential use of our newly developed method to evaluate the seam-puckering appearance objectively and quantitatively. © 2008 SPIE and IS&T.* [DOI: 10.1117/1.3041171]

1 Introduction

Sewn fabrics may often take on a puckered appearance at their seams; that is, the material may exhibit undesirable ridges, wrinkles, or corrugations. The American Association of Textile Chemists and Colorists (AATCC) has established a standard [1] (88B) that provides a set of photographs (as in Fig. 1) of five grades of puckering graded using subjective natural language terms, such as "rough." Domain experts (technicians) can use these photographs as a reference when evaluating the quality of a seam constructed using a variety of fabrics and two seam types (single-needle seams and double-needle seams). Evaluation is always done under standardized lighting and impacts not just decisions about whether sewn articles are themselves acceptable but also issues related to online adjustment of sewing machine parameters. This current nonautomated process of evaluating seam puckering, however, requires experienced employees, can be time-consuming, and can result in inconsistent or unreliable results. Attempts to improve on manual evaluation approaches have a long history going back to the 1950s. Early instruments for this purpose[2,3] used photo or displacement sensors to measure the surface contours of seams, but these sensors had numerous problems with accuracy and reproducibility. Recent computer and sensor-based approaches have used CCD cameras and 2-D image analysis techniques as well as 3-D laser scanners, which can better deal with multicolored or patterned fabrics. The 2-D imaging analysis systems are cheaper and simpler to operate than laser scanning systems, and the resolution of 2-D reflectance images is much higher than the 3-D height field; however, 2-D imaging based on single-side illumination is sensitive to illumination and texture information. Other approaches to the evaluation of seam puckering involve surface profiling and digitization and can be classified as contact or noncontact. Noncontact approaches are faster, more accurate, and more reproducible than contact methods and, thus, are the focuses of this work. There are two main noncontact methods: laser scanning and image analysis.

Laser scanning is a common method wherein laser triangulation sensors are used to determine the 3-D position of a target by measuring the reflection of its laser beam from the target surface. Kawabata and Niwa[4] used the height signal to calculate a surface roughness parameter and found that sensory evaluation of seam pucker follows the Web-Fechner law, which states that a sensory value is proportional to the logarithm of the magnitude of the quality of the physical stimulation. The resultant equation was the basis of the observation that there is an almost linear relationship between the subjective seam-pucker grade and the physical quantity. Park[5] used laser scanning to profile the seam-puckering surface and then evaluated it using neu-

Paper 08059RRR received Apr. 27, 2008; revised manuscript received Oct. 22, 2008; accepted for publication Oct. 27, 2008; published online Dec. 17, 2008.

1017-9909/2008/17(4)/043025/12/$25.00 © 2008 SPIE and IS&T.

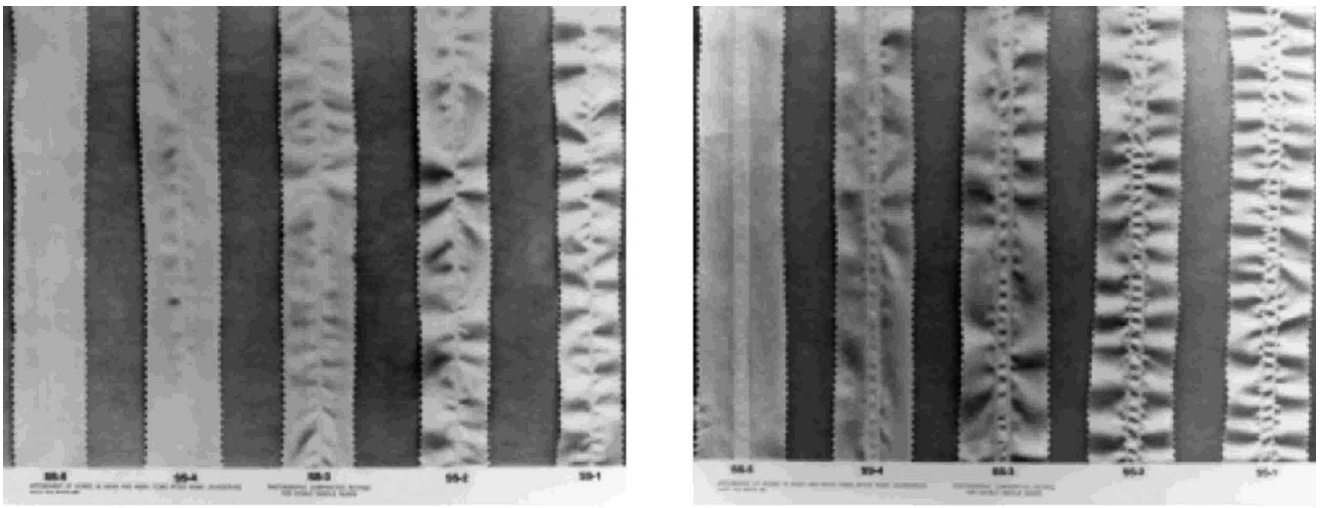

(a) (b)

Fig. 1 AATCC sample for seam gradings 5 down to 1 (a) for single needle seams and (b) for double needle seams.

ral networks. The scanning system (a displacement meter) consisting of a laser diode that could reconstruct the surface profile of the seams with little influence from color and texture. The neural network simulated human expert judgment and calculated the specific features to be used in modeling by comparing AATCC rating standards with test samples. This research shows that it is possible to predict and optimize the quality of seam pucker based on material properties and processing parameters. Fan[6] and Fan *et al.*[7] used a commercial 3-D laser scanning system consisting of a laser scanning head, robot arm, computer, and some special software for data acquisition to scan the 3-D profile of garment seams. They used the 2-D filters to obtain the 3-D pucker profiles by removing the high-frequency components in the seam profiles as these could come from individual fabric threads or from noise. They similarly removed the lower-frequency components, which might come from the smooth surface of a garment. They defined four geometrical parameters to characterize the seam pucker profile: average displacement, its variance, the skewness of the height distribution, and the kurtosis of the height distribution. They found that the logarithm of the average displacement from the mean magnitude and its variance were linearly related to the severity of seam puckering. The addition of the logarithm of the skewness and kurtosis of the height distribution made little improvement in the correlation; thus, they selected the first two parameters as the objective measures of seam puckering. In Fan[6] ten men's shirts made from different fabrics of similar weight and density were used as samples. They found that the relationship between the logarithm of variance and the technician-generated grade of seam pucker close to four parts on the sample garment, which were yoke seam, pocket seam, placket seam, and armhole seam.

A number of researchers have used image analysis methods to evaluate seam puckering. Stylios[8] developed a so-called pucker vision system, which consists of a CCD camera that captures the surface image of a puckered seam and a software program that evaluates the image features. The system was designed to capture images of two groups of seam stripes produced from the same fabric, one unstitched seam and one sewn with puckers. Using the mean reflection of the unstitched seams as a reference, the system assessed the configuration of the pucker by identifying the pucker wavelength and pucker amplitude to develop a pucker severity index. The major limitations of the system were the inconsistency of the light source and the influence of the pattern and color of the fabric. Richard[9] developed a computer-based seam-pucker measurement system that used digital image analysis to quantify seam surface irregularities. A video camera was used to capture seams in the immediate vicinity of the seam formation area. The measurement of the pucker index on a scale of 1 to 5 was very rapid, and the results were incorporated into a fabric sewability report, together with a measurement of the dynamic force of the sewing process.

Although the research in the literature facilitates the realization of automatic seam-pucker evaluation, the development of a high robust and intelligent method is under way for the benefit of both economy and accuracy. Most previous research used the laser scanning systems, which had the high cost of 3-D scanning and were not specially designed for the purpose of seam-puckering evaluation. The 2-D imaging system has the advantages of low cost and simple

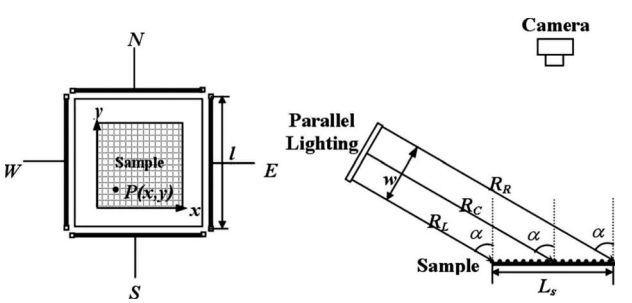

Fig. 2 X-illumination system.

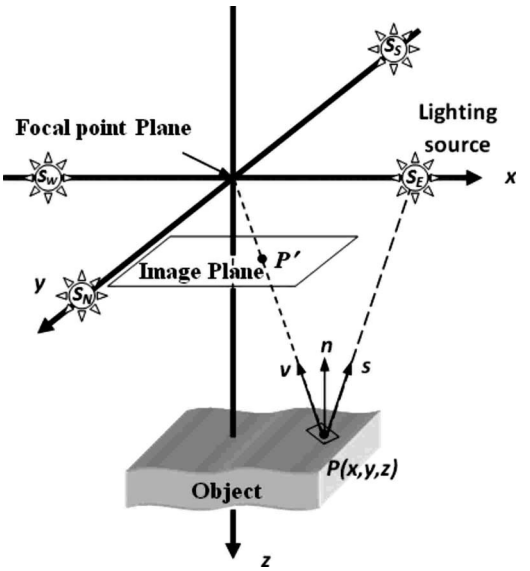

Fig. 3 Imaging geometry.

operation in comparison to the laser scanning system; the resolution of 2-D reflectance image could be much higher than 3-D height field. However, the 2-D imaging system based on one-side illumination has the limitation of being sensitive to illumination and texture information. The reason is that a 2-D reflectance image is an integration of surface profile, illumination, imaging geometry, and color/texture information; thus, one-side illumination and color/texture information have effects on the quality evaluation of seam puckering.

In addition, the seam-puckering evaluation problem could be treated as a surface roughness evaluation problem, which can be described by using the fractal analysis method; however, classical fractal dimension is not practical for the evaluation of natural objects, which is scale dependent, and thus multimorphological fractal analysis was used in our research to characterize the seam puckering appearance.

Furthermore, the Bayes classifier might be used to establish the relationship between estimated grade and those extracted features, so that a detailed quantitative description of the seam puckering appearance could be defined for the purpose of quality evaluation and measurement.

In this paper, we present a new method to automatically evaluate seam pucker that integrates X-illumination, morphological fractals, and a Bayes classifier. X-illumination is cheaper than laser scanning methods; it can also avoid the inconsistency caused by one-side illumination using the 2-D imaging analysis method. Using fractal analysis, we treat puckering as a surface-roughness evaluation problem.

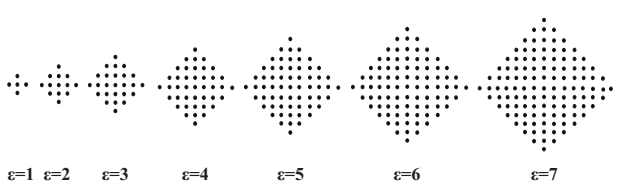

Fig. 4 SE at different scales.

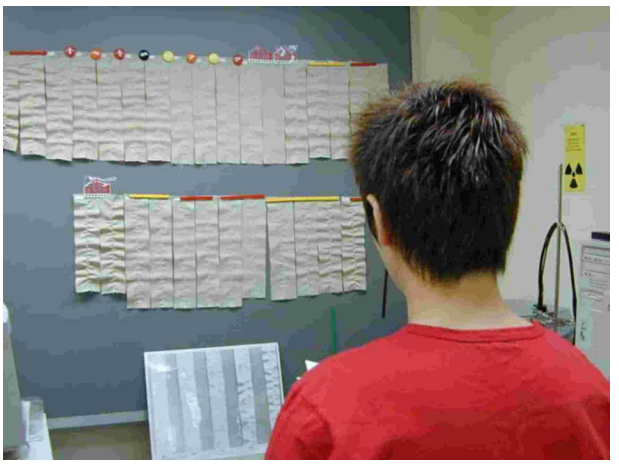

Fig. 5 Subjective evaluation of seam-puckering grade.

We do not use classical fractal dimensions because the evaluation of natural objects is scale dependent. Rather, we use multimorphological fractal analysis. Multifractal analysis has the nature of describing the surface roughness, in the consideration of the scale dependency. The Bayes classifier is used to establish the relationship between estimated grade and extracted features so as to create a detailed quantitative description of the seam puckering. The Bayes classifier is one simple and practical solution for both system training and classification, with the low cost of computing and categorizing of seam-puckering appearance.

The remainder of this paper is organized as follows. Section 2 introduces the methodology we used to characterize the seam-puckering appearance. Section 3 experimentally tests the feasibility of our presented method and investigates the color/texture effects on this method. Section 4 offers our conclusion and outlines future work.

2 Methodology

The procedure of a digital evaluation scheme for seam-puckering appearance majorly includes: data collection, feature analysis, system training, and classification. In this paper, we present an X-illumination image-acquisition system for the data collection of seam puckering appearance. X-illumination means one set of illumination units using four directional lighting resources located slantingly in the east, west, north, and south of sample testing board, which

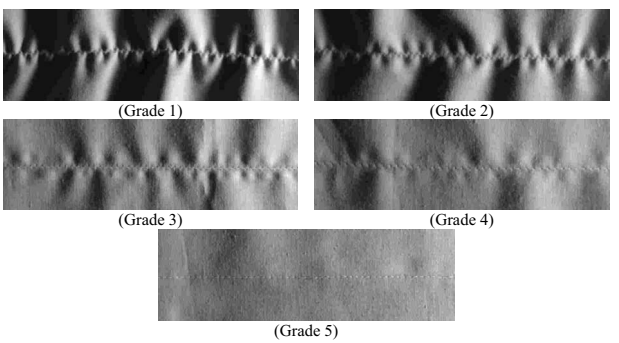

Fig. 6 Standard images of seam-puckering appearance from grades 1 to 5.

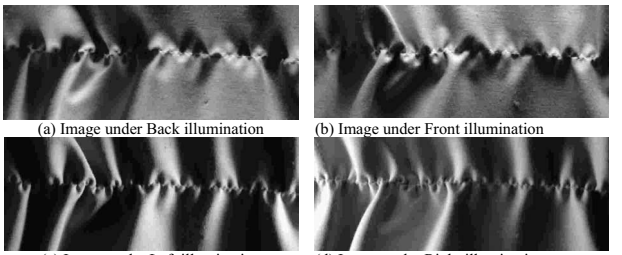

Fig. 7 Image group of four images under different illuminations (grade 1).

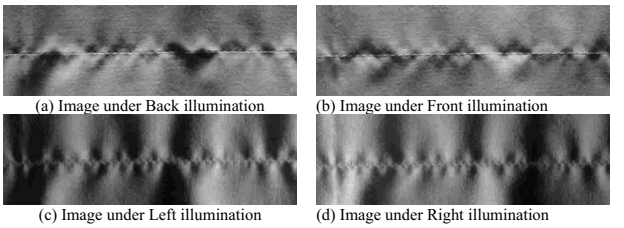

Fig. 8 Image group of four images under different illuminations (grade 2.5).

can illuminate the sample from four different directions. After that, a multimorphological fractal dimension is used for the characterization of seam-puckering degree; one set of algorithm is developed in this section. Finally, the Bayes classifier is presented for the system training and classification and the Bayes distance is used to determine the distance between testing samples and reference standards (grade 5 to 1).

2.1 *X-illumination and Imaging Geometry Setup*

An image-acquisition setup that yields gray value images preserving the seam features relevant for quality classification (mainly waviness) is crucial for a reliable and accurate judgment. Figures 2 and 3 show our proposed X-illumination and imaging geometry image-acquisition setup, which is composed of a platform for the sample seam, a digital camera, and one set of light sources located slantingly beside the platform. A lighting box containing platform and lighting sources is assembled to illuminate the test sample from four directions. The digital camera is located on top of the lighting box, which can capture an image group made up of four images with the same imaging geometry but with different incidence angles $[S_E, S_S, S_W, S_N]$. In the observing system, the vector of incidence lighting could be calculated as $S_E=[ctg\alpha, 0, -1]$; $S_S=[0, -ctg\alpha, -1]$; $S_W=[-ctg\alpha, 0, -1]$; $S_N=[0, ctg\alpha, -1]$.

2.2 *Multimorphological Fractal Dimension*

In this section, the theory of fractal model and morphological fractals is introduced and then extended to objectively estimating of the multimorphological fractal dimension for the purpose of characterization of seam-puckering appearance. The detailed calculation of the multimorphological fractal dimension is presented including the selection of structuring element, the estimation of surface area based on erosion and dilation, and the estimation of fractal dimension.

2.2.1 *Fractal model*

The central idea of fractals can be explained by considering how we might measure the surface area of a grain of sand. Obviously, the precision of measurement is controlled by the scale of measurement, because the smaller the scale, the more precise our measurement would be considering those nooks and crannies that would be visible at that smaller scale.

Fractal geometry[10] characterizes this ability of an n-dimensional object to fill the $(n+1)$-dimensional space, where the relationship of a measure M with the topological dimension n, and the scale ε is expressed as

$$M(\varepsilon) \propto \frac{1}{\varepsilon^r}, \quad 0 \leqslant r \leqslant 1, \tag{1}$$

where the quantity $r+n$ (denoted by D) is called the fractal dimension or Hausdorf-Besicovich dimension and characterizes the degree of erratic behavior. For a real object, the measure M is independent of the scale ε and, hence, $n=D$. Thus, a fractal object can be defined as a set for which the fractal dimension is greater than the topological dimension.

2.2.2 *Morphological fractals*

The digitized image of fabric seams is represented as a surface whose height represents the gray level at each point. The surface area at different scales is estimated using a series of dilations and erosions of this surface by a give-structuring element whose size determines the scale. Mathematical morphology, as developed by Serra,[11] is basically a set theory and uses a set transform for image analysis. The geometrical structure of an image could be examined by probing it with a structuring element (SE). The SE encodes primitive shape information. In a discrete approach, the shape is described as a set of vectors with respect to a particular point—the center, which does not necessarily belong to the SE. During morphological transformation, the SE is matched on the whole image and the shape-matching information could be used to define the transformation. The transformed image is thus a function of the SE distribution in the original image.

In particular, dilation of a set X with an SE Y is given by

$$X \oplus Y = \{x: Y^x \cap X \neq \phi\}. \tag{2}$$

In addition, erosion of a set X with an SE Y is given by

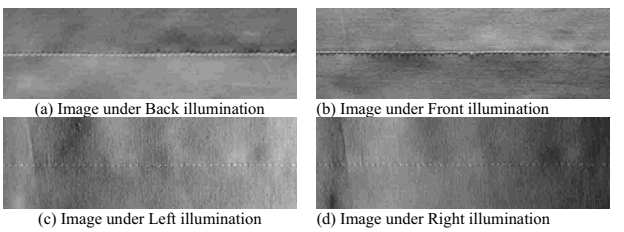

Fig. 9 Image group of four images under different illuminations (grade 5).

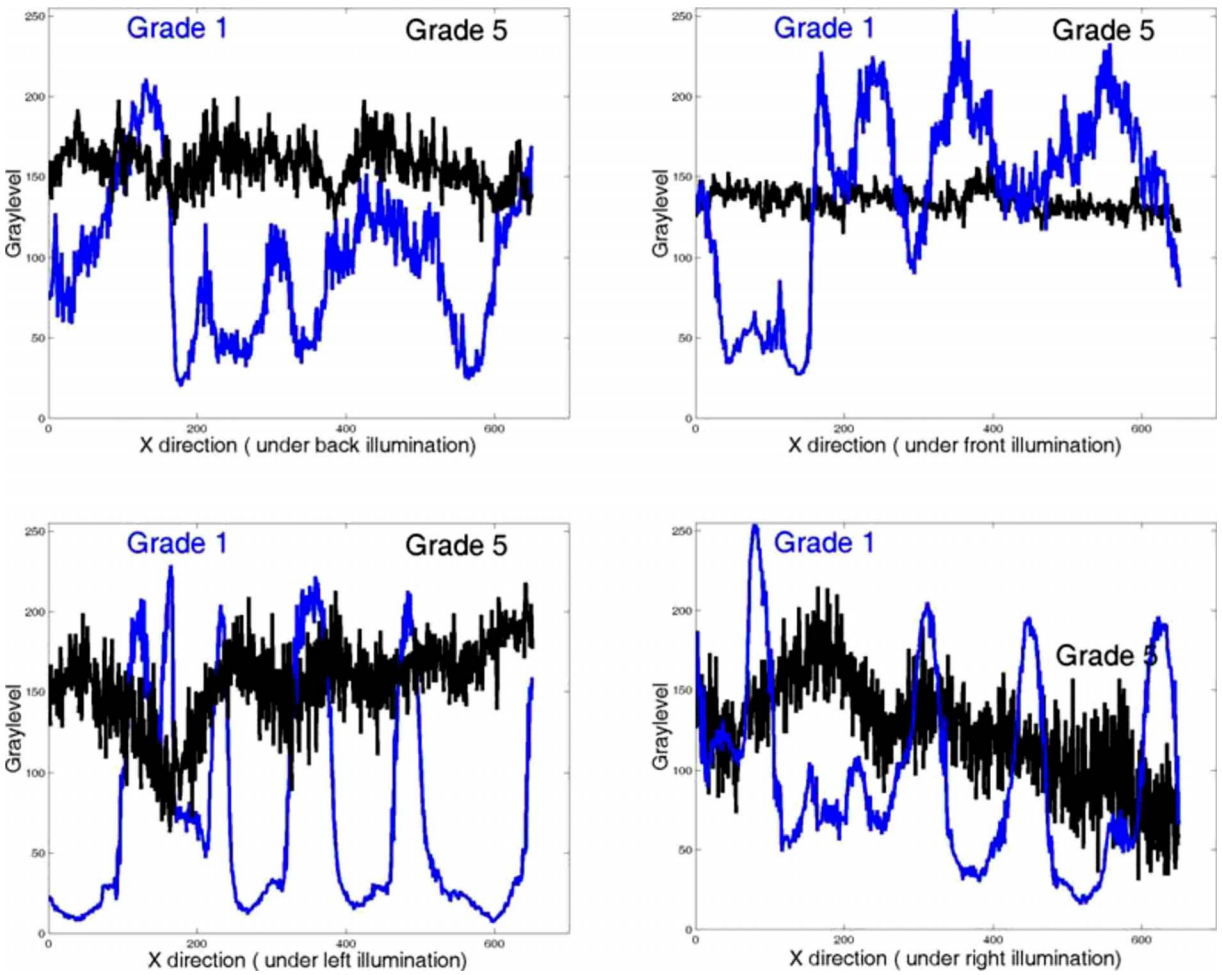

Fig. 10 Comparison of surface profiles under different illumination (grades 5 and 1).

$$X\Theta Y = \{x : Y^x \subset X\}, \tag{3}$$

where Y^x indicates the translation of set Y with x. Using the above operation, the surface area of a compact set X with respect to a compact convex SE Y that is symmetrical with respect to the origin is given by

$$S(X,Y) = \lim_{\varepsilon \to 0} \frac{V(\partial X \oplus \varepsilon Y - \partial X \Theta \varepsilon Y)}{2\varepsilon}, \tag{4}$$

where ∂X is the boundary of set X, $\oplus$ denotes the dilation of the boundary of set X by the SE Y scaled by a factor ε, and Θ denotes the erosion of the boundary of set X by the SE Y scaled by a factor ρ. $V(X)$ gives the volume of set X. It has been observed that even though for "regular" classes of sets the surface area $S(X,Y)$ is finite, for many "natural" objects, this can be infinite.

From the above expressions, it can be seen that dilating by ρ^Y hides all structures smaller than ρ^Y and, therefore, it is equivalent to looking at the surface at scale ρ. If the object is regular, then the surface area will not change with ε. For a fractal object, $S(\partial X, Y, \varepsilon)$ is increasing exponentially with decreasing ε. By taking the logarithm, we now have

$$\log[S(\partial X, Y, \varepsilon)] = \log(K) - r \log(\varepsilon), \tag{5}$$

$$D = 2 + r, \tag{6}$$

where K is the proportionality constant. D could be estimated by plotting $\log[S(\partial X, Y, \varepsilon)]$ versus $\log(\varepsilon_i)$ for a given set of scale factors ρ_i, $i = 1, 2, \ldots, N$ and calculating the gradient of the line that fits the plot.

2.2.3 *Multimorphological fractal*

The rhombus element Y is selected in this study as the basic structuring element to perform a series of dilation and erosion operations on the fabric images X. Figure 4 shows the representations of structuring elements whose scale is from $\varepsilon = 1$ to $\varepsilon = 7$, and the area of these structuring elements is 5, 13, 25, 41, 61, 85, and 113 pixels.

The series of dilation or erosion of X by εY required for the above computation can be further reduced to dilation or erosion by the unit element Y. If $X_Y^\varepsilon = X \oplus \varepsilon Y$ or $X_Y^\varepsilon = X \Theta \varepsilon Y$, then

$$X_Y^{\varepsilon+1} = X \oplus (\varepsilon + 1)Y = (X \oplus \varepsilon Y) \oplus Y = X_Y^\varepsilon \oplus Y$$

or

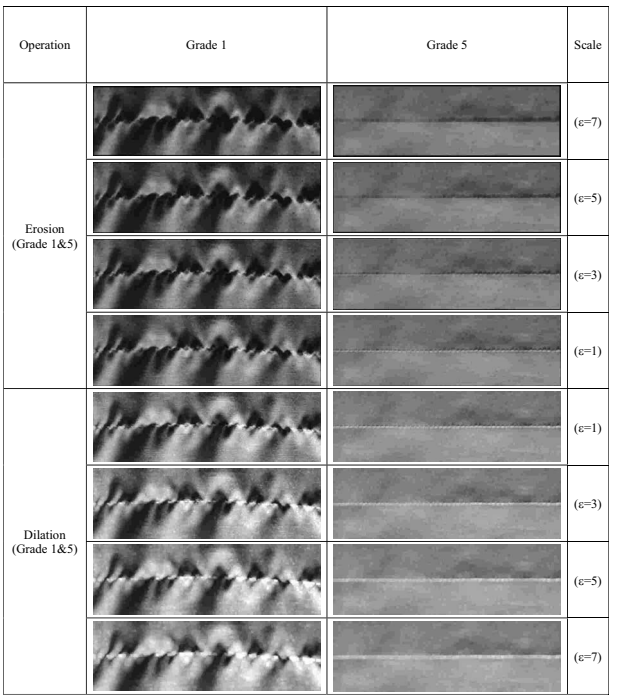

Fig. 11 Image series of standard images (grades 5 and 1) for seam-puckering appearance after seven times erosion operation and image series of standard images (grades 5 and 1) after seven times dilation operation.

$$X_Y^{\varepsilon+1} = X\Theta(\varepsilon+1)Y = (X\Theta\varepsilon Y)\Theta Y = X_Y^{\varepsilon}\Theta Y. \quad (7)$$

For experimental purposes, the surface area of a set X at scale ε is calculated as

$$S(\partial X, Y, \varepsilon) = \frac{V(\partial X \oplus \varepsilon Y - \partial X\Theta\varepsilon Y)}{2\varepsilon}. \quad (8)$$

The surface area $S(X,Y,\varepsilon_i)$ can be iteratively calculated as follows. Let the image X be defined as the set of triplets $\{\langle f(x,y); x=1,2,\ldots,n; y=1,2,\ldots,m\rangle\}$, m, n is the width and height of image and the structuring element be given as a set of triplets $\{\langle x_i, y_i, z_i\rangle, i=1,2,\ldots,P\}$. The ε'th dilate $f_\varepsilon^u(x,y)$ is calculated as

$$f_\varepsilon^u(x,y) = \max\{f_{\varepsilon-1}^u(x+x_i, y+y_i)\cdot z_i, \quad i=1,2,\ldots,P\}. \quad (9)$$

The ε'th erosion $f_\varepsilon^l(x,y)$ is calculated as

$$f_\varepsilon^l(x,y) = \min\{f_{\varepsilon-1}^l(x+x_i, y+y_i)\cdot z_i, \quad i=1,2,\ldots,P\}. \quad (10)$$

The initial condition $f_0(x,y)$ is set to $f(x,y)$. The surface area at each step can then be calculated as

$$S(X,Y,\varepsilon) = \frac{V(X,Y,\varepsilon)}{2\varepsilon} = \frac{\Sigma_{x\in[1,N],y\in[1,M]}[f_\varepsilon^u(x,y) - f_\varepsilon^l(x,y)]}{2\varepsilon}. \quad (11)$$

By taking the logarithm as seen from Eqs. (5) and (6) we can estimate D by plotting $\log[S(X,Y,\varepsilon_i)]$ versus $\log(\varepsilon_i)$ for a given set of scale factors ε_i, $i=1,2,\ldots,N$ and calcu-

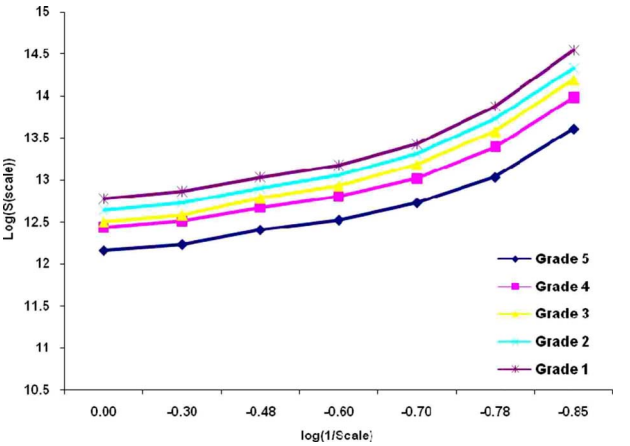

Fig. 12 Logarithmic plot of surface area S(scale) versus scale (1/scale) for five standard images from grade 1 to grade 5.

Table 1 Fractal dimension vectors estimated.

Fractal dimension under X-illumination	Grade 5	Grade 4	Grade 3	Grade 2	Grade 1
D_{left}	2.91483	2.90064	3.36794	3.39148	3.80933
D_{right}	3.46917	3.67342	3.75834	3.9559	4.06505
D_{front}	3.13162	3.26946	3.10411	3.73508	3.63244
D_{back}	3.37468	3.63619	3.75834	3.49815	3.35054
Max	**3.46917**	**3.67342**	**3.75834**	**3.9559**	**4.06505**
Min	**2.91483**	**2.90064**	**3.10411**	**3.39148**	**3.35054**
Std	**0.249616**	**0.36209**	**0.320217**	**0.252065**	**0.300599**
Mean	**3.22575**	**3.369928**	**3.497183**	**3.645153**	**3.71434**

Table 2 Fractal vectors of 24 testing specimens.

Sample No.	D_{left}	D_{right}	D_{front}	D_{back}	Max	Min	Std	Mean
1	2.9028	2.8097	3.3133	3.2606	3.3133	2.8097	0.2525	3.0716
2	3.4558	3.6625	3.6275	3.2882	3.6625	3.2882	0.1724	3.5085
3	3.2581	3.5740	3.1221	3.2152	3.5740	3.1221	0.1962	3.2923
4	3.3132	3.6043	3.6125	3.3662	3.6125	3.3132	0.1567	3.4740
5	3.3461	3.5895	3.4932	3.6453	3.6453	3.3461	0.1310	3.5185
6	3.4659	4.0296	3.7219	3.1841	4.0296	3.1841	0.3607	3.6004
7	3.3782	3.7356	3.6177	3.6528	3.7356	3.3782	0.1534	3.5961
8	3.7720	3.9830	3.6489	3.7696	3.9830	3.6489	0.1388	3.7934
9	3.1459	3.3973	3.0842	2.9174	3.3973	2.9174	0.1990	3.1362
10	3.4725	3.1859	3.1535	3.1696	3.4725	3.1535	0.1520	3.2454
11	3.4958	3.7140	3.5386	3.1955	3.7140	3.1955	0.2155	3.4860
12	3.1655	3.5240	3.6277	3.2324	3.6277	3.1655	0.2234	3.3874
13	3.3151	3.6262	3.2863	3.3645	3.6262	3.2863	0.1555	3.3980
14	3.4429	3.3403	3.3710	2.9121	3.4429	2.9121	0.2402	3.2666
15	3.0080	2.9010	2.9653	3.1491	3.1491	2.9010	0.1052	3.0059
16	3.2641	3.8320	3.3979	3.3550	3.8320	3.2641	0.2528	3.4623
17	3.4356	3.9366	3.2614	3.5850	3.9366	3.2614	0.2870	3.5547
18	3.3679	3.7615	3.4788	3.5713	3.7615	3.3679	0.1666	3.5449
19	3.8333	4.0520	3.7371	3.4637	4.0520	3.4637	0.2439	3.7715
20	3.3299	3.4280	3.1809	3.4865	3.4865	3.1809	0.1336	3.3563
21	3.4264	3.8637	3.6440	3.0818	3.8637	3.0818	0.3333	3.5039
22	3.2143	3.8924	3.6763	3.4911	3.8924	3.2143	0.2875	3.5685
23	3.0083	3.5556	3.5700	3.0161	3.5700	3.0083	0.3180	3.2875
24	3.2532	3.5680	3.5728	3.1758	3.5728	3.1758	0.2079	3.3925

lating the gradient of the line that fits the plot.

After the morphological fractal dimensions of four images under different illumination $[D_{left}, D_{right}, D_{front}, D_{back}]$ are calculated, D_{left}, D_{right}, D_{front}, D_{back} are the morphological fractal dimensions of fabric image under left-side, right-side, front-side, and back-side illumination separately; then, one feature vector,

$$\vec{V} = \begin{bmatrix} \max(D_{left}, D_{right}, D_{front}, D_{back}), \\ \min(D_{left}, D_{right}, D_{front}, D_{back}), \\ \text{mean}(D_{left}, D_{right}, D_{front}, D_{back}), \\ \text{std}(D_{left}, D_{right}, D_{front}, D_{back}) \end{bmatrix},$$

is defined to characterize the seam puckering properties.

2.3 *Bayes Classifier*

The Bayes classifier, based on Bayes distance function, is used in this paper to establish the grading system for seam-puckering appearance. The five standard seam-puckering specimens from grade 1 to grade 5 establish a feature space for the grading system. Their feature vectors $[\mathbf{V}_1, \mathbf{V}_2, \mathbf{V}_3, \mathbf{V}_4, \mathbf{V}_5]$ are calculated and used for training of the grading system. To account for the distance between one specimen and five grade clusters, we used a simplified Bayes distance function as the metric to determine "closeness." Under the conditions that the features are independent and Gaussian, the Bayes distance provides the maxi-

Table 3 Bayes distance between 24 testing specimens and 5 standard grade clusters.

Sample No	d_5	d_4	d_3	d_2	d_1	Estimated grade	Technician-generated grade
1	**0.2411**	0.4888	0.6859	1.0394	1.1283	5	4.5
2	0.5143	0.4533	**0.2551**	0.3490	0.4741	3	3
3	**0.2843**	0.3041	0.3027	0.5882	0.6945	1	1
4	0.5011	0.4764	**0.3037**	0.4030	0.5335	3	2.5
5	0.5645	0.5241	**0.3280**	0.3595	0.4933	3	3
6	0.7360	0.5102	0.3038	0.2495	**0.2134**	1	1
7	0.6591	0.5715	0.3365	**0.2466**	0.3807	2	2
8	1.0681	0.9407	0.6840	**0.3190**	0.3580	2	2
9	0.3972	**0.1233**	0.5570	0.8937	0.9890	4	3.5
10	**0.2589**	0.4050	0.4194	0.6784	0.7950	5	5
11	0.4574	0.3515	**0.1463**	0.3516	0.4546	3	3
12	0.3403	0.3030	**0.2056**	0.4754	0.5817	3	3
13	0.4498	0.4409	**0.2960**	0.4361	0.5638	3	2.5
14	**0.0522**	0.2807	0.4426	0.7978	0.8851	5	4.5
15	**0.4128**	0.6881	0.8367	1.1497	1.2574	5	4.5
16	0.5578	0.4216	**0.1918**	0.2550	0.3572	3	3
17	0.6710	0.4891	0.2468	**0.1634**	0.2239	2	2
18	0.6337	0.5431	0.3090	**0.2360**	0.3730	2	2
19	0.9707	0.7972	0.5446	**0.1746**	0.1395	2	2
20	**0.3200**	0.4072	0.3667	0.6018	0.7208	5	4.5
21	0.5193	0.2963	**0.1087**	0.3619	0.3977	3	3
22	0.6244	0.4374	**0.1905**	0.2063	0.2642	3	2.5
23	0.1761	**0.1667**	0.2977	0.6543	0.7381	4	4
24	0.3308	0.3319	0.2513	0.5090	0.6205	3	3.5

mum likelihood classification. Under these assumptions, the likelihood function for a feature vector $\bar{v}$ belonging to fabric appearance grade l is

$$p(\mathbf{V}=\mathbf{v}|\mathbf{L}=\mathbf{l})=\prod_{i=1}^{n}\frac{1}{\sqrt{2\pi}\sigma_{i,j}}e^{-[(v_i-u_{i,l})^2/2\sigma_{i,l}^2]}, \tag{12}$$

where v_i represents the elements of the feature vector, u_{il} represents the mean value of the element v_i of grade l, σ_{il} represents the standard deviation of the element v_i of grade l, and n corresponds to the total number of features. The grade classification is achieved by choosing grade l, which minimizes the simplified Bayes distance function

$$d_l=\sum_{i=1}^{n}\left[2\ln\sigma_{i,l}+\left(\frac{v_i-u_{i,l}}{\sigma_{i,l}}\right)^2\right]. \tag{13}$$

This study uses four fractal dimensions under different illuminations to make up a fractal vector, and five standard specimens from grade 1 to grade 5 were used for the system training. Each grade class only has one standard seam-puckering sample as a specimen, and thus, the Bayes distance function could be simplified as follows:

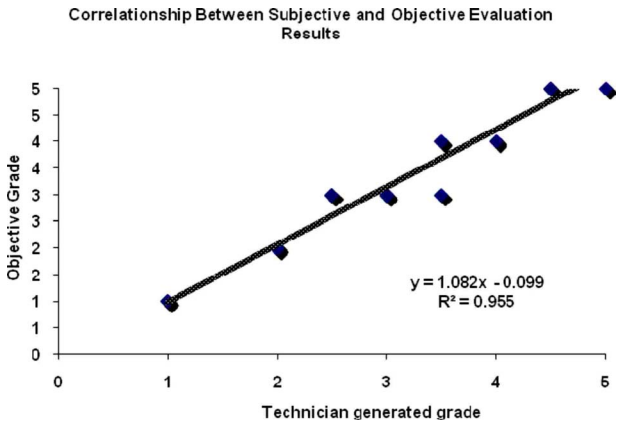

Fig. 13 Correlation between subjective and objective evaluation.

$$d_l = \sum_{i=1}^{n} (v_l - u_{i,l})^2. \tag{14}$$

After the calculation of the fractal vectors of the testing specimens and the calculation of the distances between five standard clusters and the testing specimens, the grade of each testing specimen could be determined from the grade cluster corresponding to the minimum distance value.

3 Experimental Results

3.1 *Sample preparation and subjective evaluation*

In our research, 29 samples as illustrated in Fig. 5 were made from gray cotton woven fabrics, which were sewed with different settings by adjusting the thread tension during sewing of the seams to achieve different seam-puckering grades, as illustrated in Fig. 6. Each fabric specimen was then cut into 380×120 mm; the seam-pucker grades of these samples were evaluated by a panel of 10 observers, in each case omitting the most extreme grade of the 10 obtained and then determining the average grade from the remaining eight.

3.2 *Image acquisition*

Four images of each sample were captured at a resolution of 1024×768 pixels under four different illuminating directions; the region of the image was set at 650×250 pixels for all the samples. The sample surface to be captured is 104×40 mm, thus making the image resolution 15.8 dpi. Each pixel was assigned a gray-level value from 0 for black to 255 for white. Figures 7 (grade 1), 8 (grade

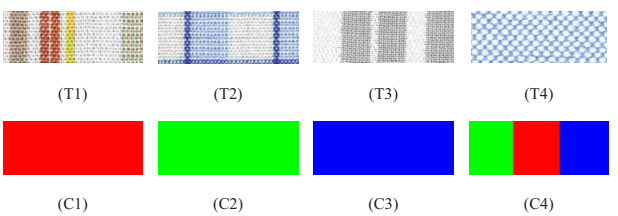

Fig. 14 Types of texture and color used for system validation. (Color online only.)

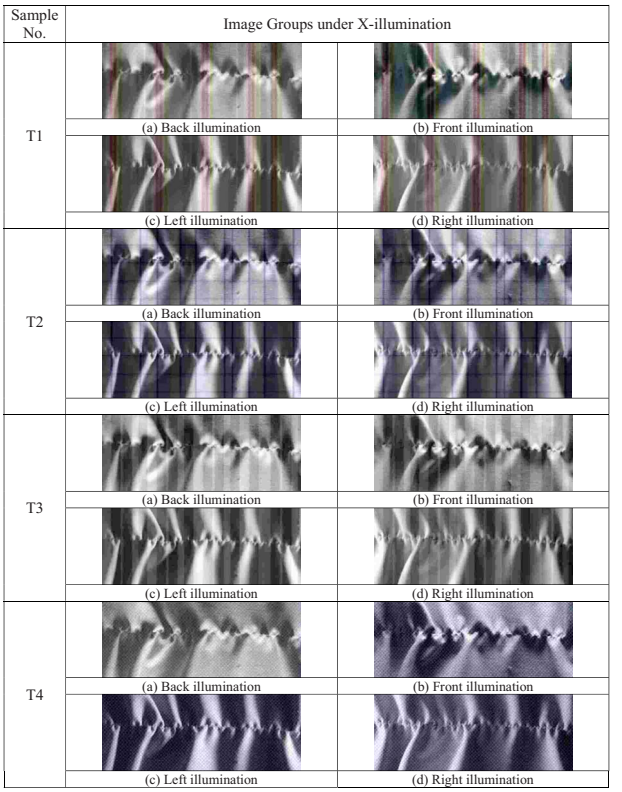

Fig. 15 Image groups under X-illumination with different texture attributes.

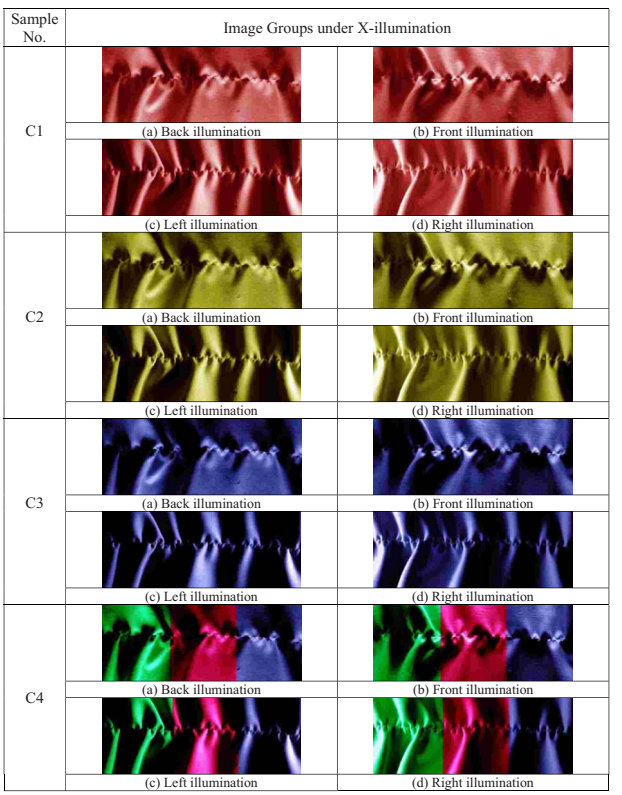

Fig. 16 Image groups under X-illumination with different color attributes.

Table 4 Fractal vectors of eight image specimens with different color and texture attribute.

Sample No.	D_{left}	D_{right}	D_{front}	D_{back}	Max	Min	Std	Mean
T1	3.8484	3.5097	4.0317	3.8629	4.0317	3.5097	3.6966	3.7882
T2	3.8303	3.6985	4.1102	4.0542	4.1102	3.6985	3.7797	3.8983
T3	3.8501	3.7067	4.1611	4.0616	4.1611	3.7067	3.8060	3.9199
T4	3.6844	3.6400	3.9940	3.8932	3.9940	3.6400	3.6728	3.7779
C1	3.6975	3.5155	4.0530	3.9959	4.0530	3.5155	3.6553	3.7905
C2	3.6089	3.5221	4.0075	3.9546	4.0075	3.5221	3.6129	3.7483
C3	3.7927	3.5364	4.1352	4.0776	4.1352	3.5364	3.7214	3.8605
C4	3.6631	3.5441	4.0114	3.9666	4.0114	3.5441	3.6395	3.7713

Sample No.	d_5	d_4	d_3	d_2	d_1	Estimated grade	Technician-generated grade
T1	0.9956	0.8339	0.5784	0.2035	**0.1972**	1	1
T2	1.2195	1.0683	0.8117	0.4336	**0.4154**	1	1
T3	1.2631	1.1041	0.8488	0.4697	**0.4361**	1	1
T4	1.0574	0.9261	0.6693	**0.2995**	0.3366	2	1
C1	1.0121	0.8458	0.5912	0.2151	**0.1939**	1	1
C2	0.9673	0.8126	0.5562	**0.1767**	0.1998	2	1
C3	1.1122	0.9322	0.6818	0.3155	**0.2504**	1	1
C4	0.9964	0.8444	0.5876	**0.2103**	0.2283	2	1

2.5), and 9 (grade 5) show three sets of fabric images under different illumination, whose appearance are rated from grade 1 to grade 5.

3.3 *Surface profile analysis*

Seam-puckering appearance with different puckering severity demonstrates different changes under different illumination; this phenomenon could be observed from the comparison of Figs. 7 (grade 1), 8 (grade 2.5), and 9 (grade 5). The seam-puckering appearance with rough surface profile has quite a different image intensity at the same position under different illuminations; however, the seam-puckering appearance with a smooth and flat surface profile has similar image intensity at the same position even under different illuminations, as illustrated in Fig. 10. This phenomenon indicates that it is possible to characterize the seam-puckering appearance using the X-illumination system.

3.4 *Multimorphological fractal analysis*

Figure 11 Image Series of Standard Images (grades 5 and 1) for seam-puckering appearance after seven times erosion operation and Image series of standard images (grades 5 and 1) after seven times dilation operation

The plotting chart of $\log[S(X,y,\varepsilon_i)]$ versus $\log(\varepsilon_i)$ for five standard images from grade 5 to grade 1 is illustrated in Fig. 12 for a given set of scale factors ε_i, $i=1,2,\ldots,N$. The gradient of the line that fits the plot was calculated to estimate the morphological fractal of these standard images.

Table 1 shows the estimated fractal dimension vectors of five standards under X-illumination. To normalize the distribution of these fractal dimensions using statistical method, the maximum/minimum/Std/mean values of these fractal dimensions under X-illumination are calculated as the descriptor of surface roughness status. It was found that the maximum and mean value have the significant correlation coefficient with the grading level.

3.5 *System Training and Grade Classification*

The five standard seam-puckering specimens from grade 1 to grade 5 were used for system training, and the other 24 specimens were used for testing.

After the calculation of the fractal vectors of 24 testing specimens as listed in Table 2 and the calculation of the distances between five standard clusters and 24 testing specimens as listed in Table 3, the grade of each testing specimen could be determined from the grade cluster corresponding to the minimum distance value.

From the results shown in Table 3 and Fig. 13, it could be found that fractal vector and Bayes distance can be used

to classify the appearance grade effectively. The estimated grades of 24 testing specimens calculated by using the Bayes classification method are close to the technician-generated grades.

3.6 *Color and Texture Effects on the Grade Classification*

The image signal is composed of four major components: imaging geometry, illumination, color and texture, and surface profile of objects. The overall perception of seam-puckering appearance should be formed through the interaction of illumination, surface profile, color/texture information, and imaging geometry, among which the imaging geometry and color/texture information could be assumed to be independent with the changing of illumination direction. Therefore, the variation of image signals should be mainly caused by the interaction of illumination and surface profile. The X-illumination system could be used to characterize the shading behavior of seam puckers by changing the illumination direction, which is quite sensitive to the degree of seam puckering. However, the color and texture information is also merged into the seam-puckering appearance. It is necessary to investigate its effects on the grade classification based on the multifractal and X-illumination method. As illustrated in Fig. 14, eight specimens with different colors or textures were selected and synthesized for this validation experiment. Figure 15 shows the image groups of four specimens under X-illumination with different texture attributes. Figure 16 shows image groups of four specimens under X-illumination with different color attributes. The seam-puckering degree of these specimens is all assigned to be grade 1. The profile of seam puckers has the nature of low frequency in the frequency domain; thus, the seam-puckering profile could be enhanced by using the low-pass filtering in our research. From the results shown in Table 4, it was found that both texture information and color information have little effect on the value of the multifractal vector. Texture has much more than color information; however, the final multifractal vector is not as sensitive to these effects and the grade classification can predict the degree of seam puckering as well. The reason behind this phenomenon lies in the integration of the complexity from texture information and surface profile information; the effects of texture information could be reduced by using the low-pass filtering method, while the surface information still could be maintained in the multifractal vector as the indicator of seam-puckering appearance.

4 Conclusion

This study has proposed an objective evaluation method for characterizing the seam-puckering appearance using X-illumination, morphological fractal analysis, and the Bayes classifier. X-illumination could provide more information about the surface profile to enhance the contrast between the seam pucker and flat background than one-side illumination. The morphological fractal method is used to characterize the surface roughness of seam puckers, which can estimate the fractal dimension of natural objects. A fractal vector is constructed to describe the degree of seam puckering instead of one single fractal. After that, a grade classifier based on Bayes distance is used to objectively determine the grades of testing samples. Our experimental results showed that a high correlation coefficient could be achieved between the estimated grades and the technician-generated grades. The color and texture effects on the grade classification were also investigated to validate our proposed method; it seems that our method is insensitive to these effects. Future studies will optimize this objective method to develop a feasible prototype for textile industry.

Acknowledgments

We acknowledge the financial support of the Hong Kong Polytechnic University and the Hong Kong Research Institute of Textile and Apparel (HKRITA).

References

1. AATCC, *Test Method 88B, Smoothness of Seams in Fabrics after Repeated Home Laundering*. AATCC, Research Triangle Park, NC (1996).
2. H. H. Hebeler and H. J. Kolb, "The measurement of fabric wrinkling," *Text. Res. J.* **20**, 650–653 (1950).
3. M. Shiloh, "The evaluation of seam pucker," *J. Text. Inst.*, **62**, 176–180 (1971).
4. S. Kawabata, M. Mori, and M. Niwa, "An experiment on human sensory measurement and its objective measurement of seam pucker level," *Int. Cloth Sci. Technol.* **9**(2–3), 203–206 (1997).
5. C. K. Park and T. J. Kang, "Objective rating of seam pucker using neural networks," *Text. Res. J.* **67**(7), 494–502 (1997).
6. J. Fan and F. Liu, "Objective evaluation of garment seams using 3-D laser scanning," *Text. Res. J.* **70**(11), 1025–1030 (2000).
7. J. Fan, D. Lu, J. M. K. Macalapine, and C. L. P. Hui, "Objective evaluation of pucker in three-dimensional garment seams," *Text. Res. J.* **69**(7), 467–472 (1999).
8. G. Stylios and J. O. Sotomi, "Investigation of seam pucker in lightweight synthetic fabrics as an aesthetic property. Part I: A cognitive model for the measurement of seam pucker," *J. Text. Inst.* **84**, 601–610 (1993).
9. C. Richard, "Pucker as fabric-thread machine mechanical instability phenomenon," *J. Fed. Asian Prof. Textile Assoc.* **3**(1), 83 (1995).
10. B. B. Mandebrot, *Fractals, Form, Chance and Dimension*, Freeman, San Francisco (1977).
11. J. Serra, *Image Analysis and Mathematical Morphology*, Academic Press, New York (1982).

Binjie Xin received his BA in textile engineering from Qingdao University in 1996 and his MS in textile material from Donghua University, China in 1999. He is currently a research associate at the Hong Kong Polytechnic University. His research is focused on the application of image analysis and artificial intelligence in the textile field.

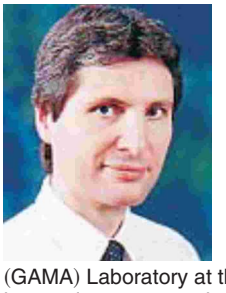

George Baciu holds degrees in computer science and applied mathematics and a PhD in systems design engineering from the University of Waterloo, where he has been a member of the Computer Graphics Lab and the Pattern Analysis and Machine Intelligence Group. He is currently a professor in the Department of Computing at the Hong Kong Polytechnic University. He serves as the founding director of the Graphics and Multimedia Applications (GAMA) Laboratory at the Hong Kong Polytechnic University, where he continues research in 3-D motion capture, motion analysis and synthesis, 3-D geometric modeling, and network graphics. He has published more than 50 academic research papers and has served as chair or cochair of international conference committees such as Game Technology Conference (GTEC), Pacific Graphics, Virtual Reality Software and Technology (VRST), Eurographics, Computer Graphics International, CAD/Graphics, and Computer Animation and Social Agents (CASA). He is a member of the IEEE and the

ACM. He was a faculty member in the Computer Science Department at the Hong Kong University of Science and Technology (HKUST) in 1993 and initiated one of the first graduate and undergraduate computer graphics curricula in Hong Kong. He was the founding director of the Graphics and Music Experimentation (GAME) Laboratory at HKUST, where he conducted research in motion synthesis, 3-D user interfaces, rendering, geometric modeling, and animation.

Jinlian Hu is a professor in the Institute of Textile and Clothing at the Hong Kong Polytechnic University. She received her PhD at UMIST, Manchester, UK in 1994. She is a fellow of Textile Institute (1998) and a fellow of Hong Kong Institution of Textiles and apparel (2000). Her research is focused on smart material, textile structure and mechanics, cloth simulation, computer vision, and artificial intelligence.